Structural Analysis of Historical Constructions – Jerzy Jasieńko (ed)
© 2012 DWE, Wrocław, Poland, ISSN 0860-2395, ISBN 978-83-7125-216-7

ON THE MIXED COLLAPSE MECHANISM OF SEMI-CIRCULAR MASONRY ARCHES

Rizzi Egidio[1], *Colasante Giada*[2], *Frigerio Annalisa*[3], *Cocchetti Giuseppe*[4]

ABSTRACT

Starting from classical Heyman's studies on the purely-rotational collapse mode of circular masonry arches, the hypothesis that friction is high enough to prevent sliding among the blocks, implying no sliding failure, is released. The onset of sliding is ruled by a classical Coulomb's static friction law. The influence of the friction coefficient on the collapse mechanism is analysed, both analytically and numerically, by locating instances of purely-rotational, mixed sliding-rotational and purely-sliding mechanisms. A doubly built-in, symmetric, complete semi-circular masonry arch subjected only to its own weight is considered. The characteristic values of the friction coefficient that limit the ranges associated to each collapse mode are identified. Analytical formulas are provided to estimate the geometrical parameters that define the limit equilibrium states of the arch, in primis the minimum thickness to radius ratio. These formulas, starting from the analysis of the classical instance of purely-rotational collapse, make new explicit reference to the mixed sliding-rotational collapse mechanism. The obtained results are compared consistently to those available in the literature.

Keywords: *Semi-circular masonry arches, Couplet-Heyman problem, Collapse mechanisms, Mixed sliding-rotational mode, Coulomb friction, Limit Analysis*

1. INTRODUCTION

Rational studies on the statics of masonry arches were blooming in 1700 with the development of the so-called pre-elastic theories; in recent times, they have culminated in the second half of 1900 in the modern application of Limit Analysis to masonry constructions, according to the pioneering work by Jacques Heyman [1-3]. Specifically, Heyman has stated three classical behavioural assumptions of masonry structures (1 – no tensile strength; 2 – infinite compressive strength; 3 – friction high-enough to prevent sliding) and investigated analytically the five-hinge *purely-rotational collapse mechanism* of continuous symmetric circular masonry arches under self-weight (taken as uniformly-distributed along geometrical centreline, with self-weight per unit length w), by providing analytical formulas for the determination of characteristic parameters, such as (Figs. 1a, b): angular position β of the inner hinge at the haunches, critical thickness to radius ratio $\eta = t / r$, non-dimensional horizontal thrust $h = H / (wr)$ acting in the limit state of minimum thickness still able to sustain the arch (*Couplet-Heyman problem*).
Such classical problem in the statics of masonry arches has been revisited within a research project that was started at the University of Bergamo in 2006 [4-10]. Arches of general half-angle of embrace $0 < \alpha < \pi$ have been analysed systematically in analytic terms and different solutions have been derived and explored numerically, which appeared consistent with recent outcomes from a re-discussion by Heyman [3] and prior developments by Ochsendorf [11-12], as well as with classical

[1] Professor, Università di Bergamo, Facoltà di Ingegneria (Dalmine), Dipartimento di Progettazione e Tecnologie, viale G. Marconi 5, I-24044 Dalmine (BG), Italy, Corresponding Author, egidio.rizzi@unibg.it
[2] Former student, Università di Bergamo, Facoltà di Ingegneria (Dalmine), Dipartimento di Progettazione e Tecnologie, viale G. Marconi 5, I-24044 Dalmine (BG), Italy
[3] Former student, Università di Bergamo, Facoltà di Ingegneria (Dalmine), Dipartimento di Progettazione e Tecnologie, viale G. Marconi 5, I-24044 Dalmine (BG), Italy
[4] Professor, Università di Bergamo, Facoltà di Ingegneria (Dalmine), Dipartimento di Progettazione e Tecnologie, viale G. Marconi 5, I-24044 Dalmine (BG), Italy;
Politecnico di Milano, Dipartimento di Ingegneria Strutturale, piazza L. da Vinci 32, I-20133 Milano, Italy

earlier work by Milankovitch [13]. An account on that has been provided in the last SAHC10 conference [6]. Lately, new developments on the role of friction have been attempted [9-10], as re-elaborated and reported here, by releasing Heyman's hypothesis 3 of no sliding failure and accounting for both *mixed sliding-rotational* and *purely-sliding collapse mechanisms* (Figs. 1c, d).

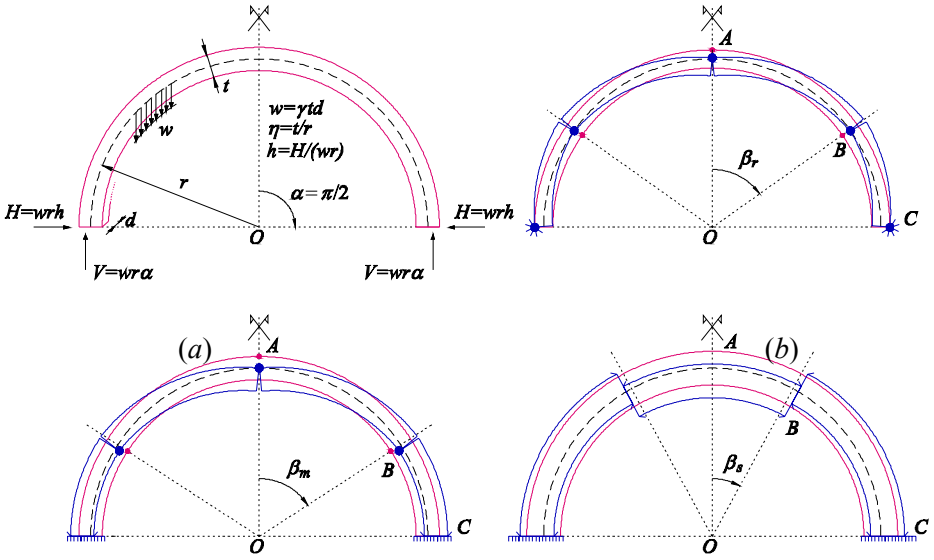

Fig. 1 Sketches of a semi-circular masonry arch under self-weight: (a) characteristic parameters; (b) purely-rotational collapse mechanism; (c) mixed sliding-rotational collapse mechanism; (d) purely-sliding collapse mechanism

Specifically, the limit values of Coulomb friction coefficient $\mu = \tan\varphi$, at the theoretical joints of the continuous arch, marking the transitions between the three collapse mechanisms in Figs. 1b-d are derived here, together with the dependence of the mixed-mode collapse characteristics (Fig. 1c) as a function of friction coefficient μ, i.e. $\beta_m(\mu)$, $\eta_m(\mu)$, $h_m(\mu)$. It is shown that, at decreasing friction coefficient μ in the arch, the horizontal thrust $h_m(\mu)$ under mixed mode is fixed (decreasing linearly) by friction and this induces non-linear increasing dependencies of $\eta(\mu)$ and $\beta(\mu)$. In other words, at decreasing friction coefficient at the joints of the arch, an increase in the critical value of least thickness is required to warrant equilibrium. Here, reference is made to full semi-circular arches with opening $2\alpha = \pi$ (Fig. 1a). The friction range in which mixed-mode collapse is shown to appear is quite narrow, in practical terms, i.e. with friction angles φ between around 22° and 17° ($\mu = \tan\varphi$ between around 0.4 and 0.3).

The present analytical and numerical results appear to be consistent to the few developed recently in the literature concerning specifically the effects of friction in masonry arches. Gilbert et al. [14] have investigated numerically the role of friction, by estimating for a semi-circular arch a minimum thickness to radius ratio $\eta = 0.1068$ in the presence of a purely-rotational collapse mechanism, when μ is greater than 0.396 (friction angle larger than $\varphi = 21.60°$). This marks, at decreasing friction, the transition from the purely-rotational to the mixed sliding-rotational mode. Furthermore, a value of $\mu = 0.31$ ($\varphi = 17.22°$) is found in [14], which locates then the shift from the mixed sliding-rotational mode to the purely-sliding mechanism. In [14] a diagram depicts the critical value of η as a function of friction coefficient μ, with a double kink at these two critical values of μ, a constant value of η for $\mu > 0.396$ and rapidly-growing values of η right on $\mu = 0.31$. These outcomes appear in good agreement with earlier results developed numerically by Sinopoli et al. [15-16], which locate the above-mentioned kinks respectively at $\mu = 0.395$ ($\varphi = 21.55°$) and $\mu = 0.309$ ($\varphi = 17.17°$). Here, the following "exact" analytical results will be consistently derived: $\mu_{rm} = 0.395832$ ($\varphi_{rm} = 21.5952°$), for the transition from purely-rotational to mixed sliding-rotational mechanisms; $\mu_{ms} = 0.309215$ ($\varphi_{ms} = 17.1824°$), for the transition between mixed and purely-sliding modes.

In the present paper, two sorts of analyses on the role of friction in masonry arches are carried-out, as presented respectively in Sections 2 and 3, with consistent results, as outlined in Section 4. First, an analytical approach in the wake of previous new analytical solutions [6-8] is developed, towards the characterisation of the mixed sliding-rotational collapse mode and relevant friction bounds. This

analysis starts from the presumed purely-rotational collapse mode due to Heyman [1-2] and, by decreasing friction, derives, through a static approach, the mechanisms that subsequently arise. Second, a comprehensive numerical approach is developed, which implements an optimisation analysis in the sense of the lower bound (static) theorem of Limit Analysis, within a commercial spreadsheet wherein an optimisation tool is available. Here, the constitutive behaviour of the circular masonry arch is stated and equilibrium conditions are varied towards the determination of the least thickness condition and attached collapse mode. Thus, the collapse mechanism, whether purely-rotational, mixed sliding-rotational or purely-sliding, is then recovered numerically, through the optimisation process, with outcomes that are fully coherent to those from the previous theoretical analysis and also to the above-quoted results from the literature [14-16].

2. ANALYTICAL APPROACH

Starting from the analysis of purely-rotational collapse in the so-called *Couplet-Heyman problem* [1-2], the determination of characteristics β, η, h for a symmetric circular arch of general half-opening α (Figs. 1a, b) may be stated in terms of the solution of the following system of three equations [6-8]:

$$\begin{cases} h = h_1 = \dfrac{(2-\eta)\,\beta\sin\beta - 2(1-\cos\beta)}{2+\eta-(2-\eta)\cos\beta} \\ h = h_2 = A - \dfrac{2}{2+\eta}, \quad A = \alpha\cot\dfrac{\alpha}{2} \\ h = h_e = \dfrac{(2-\eta)(\sin\beta+\beta\cos\beta)-2\sin\beta}{(2-\eta)\sin\beta} = \beta\cot\beta - \dfrac{\eta}{2-\eta} \end{cases} \tag{1}$$

Eqs. (1)a and (1)b represent two equilibrium relations, respectively the rotational equilibrium of any upper portion AB of the half-arch (symmetry conditions apply here) with respect to the inner intrados hinge at haunch B and of the whole half-arch AC with respect to the extrados hinge at shoulder C (Fig. 1b); Eq. (1)c corresponds to the tangency condition of the true line of thrust (locus of pressure points) at haunch intrados B and may be derived from the stationary condition $h_1'(\beta) = 0$ [7].
At variable half-opening angle α (thus $A = \alpha\cot\alpha/2$), the solution of system (1) can be developed analytically, by showing that triplet $A(\beta)$, $\eta(\beta)$, $h(\beta)$ is actually a double-valued function of inner hinge position β [7]. For the complete semi-circular arch, i.e. $\alpha = A = \pi/2$, system (1) renders directly the following characteristic solution triplet for the purely-rotational collapse mode:

$$\beta_r = 0.951141\,rad = 54.4963°, \quad \eta_r = 0.107426, \quad h_r = 0.621772 \qquad (\alpha = \pi/2) \tag{2}$$

The solution above holds true in Heyman's sense for high values of friction coefficient $\mu = \tan\varphi$ apt to prevent any sliding. By imaging now to decrease μ (not present in system (1)) from such high values, one seeks when, and where in the arch, a first sliding joint may appear, for a critical value of $\mu = \mu_{rm}$ marking the transition between purely-rotational and mixed sliding-rotational modes. This should occur when limit condition $T/N = \pm\mu$ is reached for the first time, where $T(\beta)$ and $N(\beta)$ are the shear (clock-wise positive) and normal (compression positive) components of the internal thrust force at each theoretical joint of the arch. From the translational equilibrium of any upper portion AB of the half-arch of general half-opening β, one gets, in non-dimensional terms:

$$\begin{cases} t(\beta) = \dfrac{T(\beta)}{wr} = h\sin\beta - \beta\cos\beta \\ n(\beta) = \dfrac{N(\beta)}{wr} = h\cos\beta + \beta\sin\beta \end{cases} \tag{3}$$

It may be noticed that $t(\beta)$ and $n(\beta)$ are just functions of geometrical variable β, at a given value of horizontal thrust h (which is constant along the arch). Specifically, thickness parameter η does not intervene in Eqs. (3). At the extremes of the semi-circular arch (crown A and shoulder C) one has, respectively: $\beta = 0$, $t = 0$, $n = h$, thus $t/n = 0$; $\beta = \alpha = \pi/2$, $t = h$, $n = \pi/2$, thus $t/n = 2h/\pi$.

The variation of local slope t / n of the internal thrust (to the local joint normal) can then be plotted at variable half-opening β of upper portion AB, for fixed values of h. From that, it can be noticed that absolute maxima of thrust slope are always attained at the shoulder ($\beta = \alpha = \pi/2$); relative minima (maxima on negative side) occur at stationary points in intermediate locations $0 \le \beta \le 0.5$, at variable $0 \le h \le 1$. This shows, on one hand, that the first sliding joint, at decreasing μ, should appear at the shoulder when $t / n = 2h / \pi = +\mu$, which provides transition mark $\mu = \mu_{rm}$ at $h = h_{rm} = h_r$ and then fixes the thrust in the arch $h = h_m(\mu)$ under mixed sliding-rotational mode, as linearly-decreasing with friction coefficient μ:

$$\mu_{rm} = \frac{h_r}{\pi/2} = \frac{2}{\pi} h_r = 0.395832 \ (\varphi_{rm} = 21.5952°), \ h_{rm} = h_r = 0.621772; \quad h_m(\mu) = h_\mu(\mu) = \alpha\mu = \frac{\pi}{2}\mu \qquad (4)$$

On the other hand, in seeking the stationary points in the t / n curves, one then searches for the additional joint where further sliding may occur. Then, the stationary condition $(t / n)'$ is analysed and since such sliding joint is activated when $t / n = -\mu$ and $h = h_\mu = \pi/2 \ \mu$, one gets position $\beta = \beta_s$ of the new sliding joint, at transition friction coefficient μ_{ms} and associated thrust $h_{ms} = \alpha\mu_{ms}$:

$$\beta_s = 0.499796 \, rad = 28.6362°, \quad \mu_{ms} = 0.309215 \quad (\varphi_{ms} = 17.1824°), \quad h_{ms} = 0.485714 \qquad (5)$$

At this stage, the friction boundaries for the appearance of the mixed sliding-rotational mode have been located. At $\mu = \mu_{rm}$ any 2-dof linear combination of 1-dof mechanisms in Figs. 1b and 1c is possible; at $\mu = \mu_{ms}$ any 2-dof linear combination of 1-dof mechanisms in Figs. 1c and 1d is possible. In the range $\mu_{ms} < \mu < \mu_{rm}$, the mixed-mode mechanism in Fig. 1c is found, with variable position $\beta_m(\mu)$ of inner hinge B, thickness to radius ratio $\eta_m(\mu)$ and horizontal thrust $h_m(\mu)$, at variable friction coefficient μ. This is ruled by a new system of governing equations, in place of system (1), in which second equilibrium Eq. $(1)_b$ is replaced by sliding equation $h = h_\mu = \alpha\mu$, namely:

$$\begin{cases} h = h_1(\eta, \beta) \\ h = h_\mu(\alpha, \mu) = \alpha\mu \qquad (\alpha = \pi/2) \\ h = h_e(\eta, \beta) \end{cases} \qquad (6)$$

The solution of this system is somehow similar to that developed for the purely-rotational mode [7] and leads to trends $\eta_m(\mu)$, $\beta_m(\mu)$, $h_m(\mu)$ (Figs. 3-4, Section 4), delimited on the left by characteristics β_{ms}, η_{ms}, h_{ms} at $\mu = \mu_{ms}$:

$$\beta_{ms} = 1.05616 \, rad = 60.5134°, \quad \eta_{ms} = 0.200637, \quad h_{ms} = 0.485714 \qquad (7)$$

Tab. 1 below reports the analytically-evaluated ("exact") mixed-mode collapse characteristics β, η, h at variable friction coefficient μ. The present analytical outcomes are further commented in Section 4, with comparison as well to independent, matching, numerical results, as derived in the next section.

Table 1 "Exact" critical values of η, h, β obtained by the analytical analysis at variable friction coefficient μ.
Sliding joints appear at β = π / 2 rad = 90° for 0.309215 = $\mu_{ms} \le \mu \le \mu_{rm}$ = 0.395832
and at β = β_s = 0.499796 rad = 28.6362° for μ = μ_{ms} = 0.309215

μ	η	h	β [rad]	β [deg]	μ	η	h	β [rad]	β [deg]
0.7	0.107426	0.621772	0.951141	54.4963	0.35	0.152920	0.549779	1.01227	57.9986
0.3959	0.107426	0.621772	0.951141	54.4963	0.34	0.163977	0.534071	1.02392	58.6661
0.395832	0.107426	0.621772	0.951141	54.4963	0.33	0.175448	0.518363	1.03499	59.3003
0.3958	0.107455	0.621721	0.951188	54.4991	0.32	0.187338	0.502655	1.04548	59.9016
0.39	0.112750	0.612611	0.959654	54.9841	0.31	0.199653	0.486947	1.05540	60.4702
0.38	0.122192	0.596903	0.973737	55.7910	0.3093	0.200531	0.485847	1.05608	60.5088
0.37	0.132031	0.581195	0.987190	56.5618	0.309215	0.200637	0.485714	1.05616	60.5134
0.36	0.142273	0.565487	1.00003	57.2974	0.3092	No equilibrium solution			

3. NUMERICAL APPROACH

A numerical algorithm for the study of the collapse mechanisms of symmetric circular masonry arches has been created within commercial spreadsheet *Excel* [4, 9, 10]. It makes use of an optimisation function named *"Solver"*, which allows for the selection of a GRG (Generalised Reduced Gradient) engine, towards the solution of smooth non-linear optimisation problems. Input is constituted here by two kinds of data:

- geometrical: arch width d, mean radius r (both nominally fixed to 1 m);
- material: limit tension stress σ_t (set to zero, according to Heyman's hypothesis 1), limit compression stress σ_c (set to 1000 kN/m^2, i.e. a high value apt to comply with Heyman's hypothesis 2), variably-fixed friction coefficient μ, weight per unit volume γ (set to 25 kN/m^3).

Based on these data, the trends of internal actions $N(\beta)$, $T(\beta)$, $M(\beta)$ along the arch are recovered by equilibrium and confronted to limit values that define section resistance, specifically in terms of shear force T and moment M. Then, an iterative procedure is put in place at variable thickness t, which is the cell variable in the optimisation process, to evaluate the limit condition of least thickness. Characteristics β (angular position of rupture joints), η, h in the limit condition are then obtained, together with the variation of internal actions $N(\beta)$, $T(\beta)$, $M(\beta)$ in the arch, and associated thrust-line eccentricity $e(\beta) = M / N$ from geometrical centreline.

The analysis is carried-out here on a complete semi-circular masonry arch (angle of embrace $2\alpha = \pi$). Due to symmetry, only one half of the arch is considered, with hyperstatic actions (moment $X = M_A$ and horizontal thrust $Y = H$) acting at geometrical centreline at crown section A. Statically-admissible configurations are the ones that warrant equilibrium of any upper portion of the arch of angular opening β. They are described in non-dimensional terms by expressions (3), which determine shear $T(\beta) = t(\beta)\, wr$ and normal $N(\beta) = n(\beta)\, wr$ actions in each theoretical section of the arch, and by the following expression of moment $M(\beta) = m(\beta)\, wr^2$. Consistently to relations (3), in non-dimensional terms:

$$m(\beta) = \frac{X}{wr^2} + h\ (1-\cos\beta) - \left(\beta \sin\beta - (1-\cos\beta)\right) \tag{8}$$

Cross section resistance may be set as follows. Given that $0 = \sigma_t\, t\, d \le N(\beta) \le \sigma_c\, t\, d$ should be always satisfied in the arch, focus is made on moment and shear resistances. Since eccentricity $e(\beta) = M(\beta) / N(\beta)$, with $N(\beta) > 0$ for $h > 0$ (compression), should not exceed $\pm\, t/2$ (no tensile strength) and assuming that shear is limited by a Coulomb's friction law with friction coefficient μ, one states the following two resistance inequalities:

$$\left|M(\beta)\right| \le N(\beta)\frac{t}{2}; \qquad \left|T(\beta)\right| \le \mu\, N(\beta) \tag{9}$$

In the optimisation process towards the determination of least thickness t_{min} still making the whole equilibrium possible, cell constraints are then represented by resistance conditions (9) and by the enforcement that, at crown section A, $Y = H > 0$ and $|X| = |M_A| \le Y\, t/2$. Equilibrium values of $N(\beta)$, $T(\beta)$, $M(\beta)$ from Eqs. (3) and (8) are determined at discretised angular positions, with angle-step $\Delta\beta = 0.001\ rad$. Optimal search of t_{min} is done iteratively by varying the initial values of $X = M_A$, $Y = H$ and t, in order to satisfy all given constraints (with tolerances in the order of 10^{-6}). Rotational and sliding joints are respectively detected, and their angular position β recorded, when limit conditions $(9)_a$ and $(9)_b$, with numerical equalities, are reached (Fig. 2).

A high value of friction coefficient is set first, namely $\mu = 0.7$ ($\varphi \cong 35°$), which should allow for predicting a purely-rotational collapse mode, due to Heyman's hypothesis 3. The analysis is then repeated at lowering values of friction coefficient μ, which has been reduced by steps up to $\Delta\mu = 0.0001$, until the numerical algorithm was no-longer able to find equilibrium solutions. Transition conditions at $\mu = \mu_{rm}$ and $\mu = \mu_{ms}$ have been found numerically, by looking at activated hinge and/or sliding joints (Fig. 2). Results have been recorded in terms of characteristic parameters β, η, h at variable μ [9]. Salient numerical results are reported in Tab. 2 below (to be compared to analytical results in earlier Table 1).

It may be noted from Table 2 that for $\mu = 0.3959$ ($\varphi = 21.5986°$) the algorithm detects numerically the simultaneous presence of a rotational and a sliding joint at $\beta = \alpha = 90°$. This provides a consistent

numerical estimate of "exact" friction coefficient $\mu_{rm} = 0.395832$ ($\varphi_{rm} = 21.5952°$), as derived earlier analytically. Further, the lack of equilibrium solutions for $\mu < 0.3093$ ($\varphi < 17.1868°$) provides a consistent numerical approximation of "exact" bound $\mu_{ms} = 0.309215$ ($\varphi_{ms} = 17.1824°$). These numerical results are also consistent with previous numerical outcomes in [14-16], as cited in the Introduction. Also, approximate numerical values of characteristic parameters β, η, h fit quite well with "exact" predictions from the analytical approach (Tab. 1), as analysed, represented and resumed next.

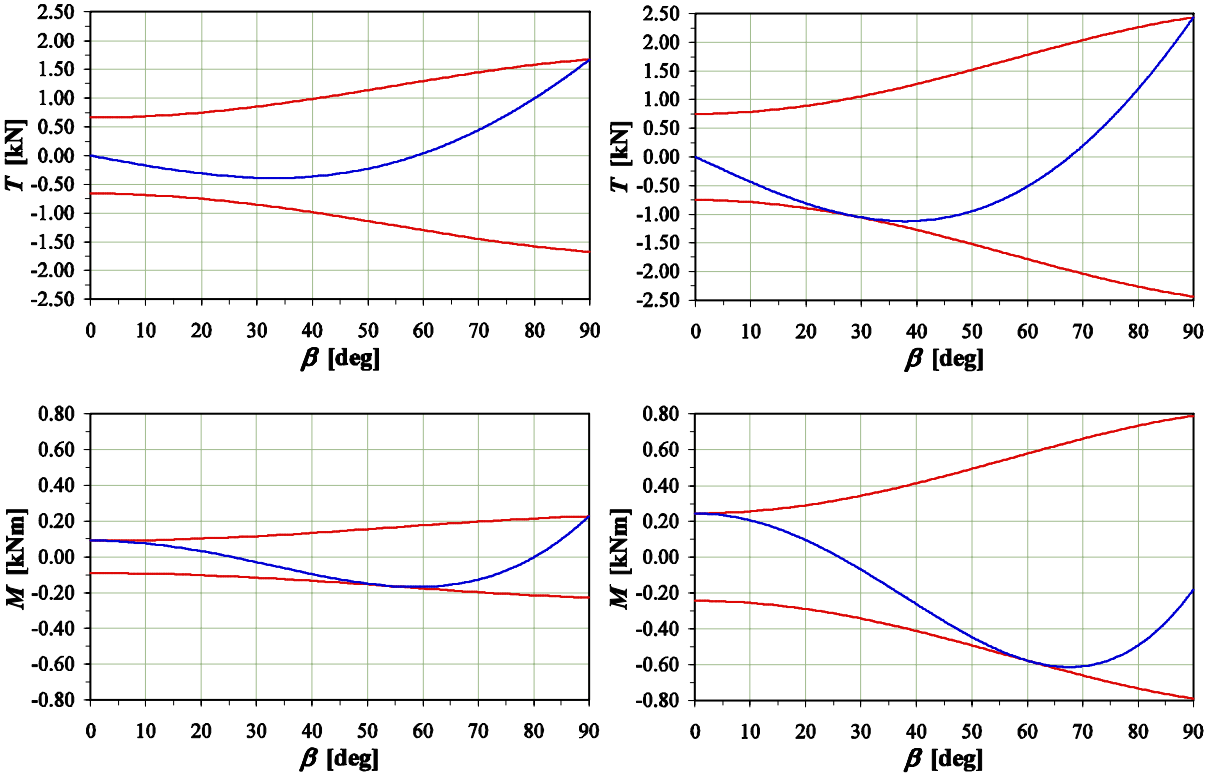

Fig. 2 Numerical optimisation results for the trends of shear T(β) and moment M(β) at friction coefficients: (a) μ = 0.3959; (b) μ = 0.3093

Table 2 Approximate critical values of η, h, β obtained by the numerical analysis at variable friction coefficient μ

μ	η	h	Hinge joints β [deg]	Sliding joints β [deg]	μ	η	h	Hinge joints β [deg]	Sliding joints β [deg]
0.7	0.107426	0.621772	0-54.4883-90	-	0.35	0.152920	0.549779	0-58.0120	90
0.396	0.107426	0.621772	0-54.4883-90	-	0.34	0.163977	0.534071	0-58.5563	90
0.3959	0.107663	0.621878	0-54.4883-90	90	0.33	0.175448	0.518363	0-59.3011	90
0.3958	0.107456	0.621721	0-54.4883	90	0.32	0.187338	0.502655	0-59.9027	90
0.39	0.112750	0.612611	0-54.9753	90	0.31	0.199653	0.486947	0-60.5043	90
0.38	0.122191	0.596903	0-55.7774	90	0.3094	0.200406	0.486004	0-60.5043	90
0.37	0.132031	0.581195	0-56.6082	90	0.3093	0.200531	0.485847	0-60.5043	28.6479-90
0.36	0.142273	0.565487	0-57.2958	90	0.3092	No equilibrium solution			

4. SUMMARY OF ANALYTICAL AND NUMERICAL OUTCOMES

Figs. 3-4 resume together the present analytical and numerical results, by showing the classical characteristics η, β, h at variable friction coefficient μ. Numerical data are over-scored with crosses on continuous analytical trends (parametric plots), with very good matching among them.

On the hierarchy of collapse mechanisms at variable (decreasing) μ, it may be resumed that for $\mu > \mu_{rm}$ the collapse mechanism in the least thickness condition is purely-rotational (Fig. 1b). Characteristics β, η, h remain unvaried at changing μ: since purely-rotational collapse is uniquely determined by arch geometry, they are not dependent on values of friction coefficient greater than μ_{rm}.

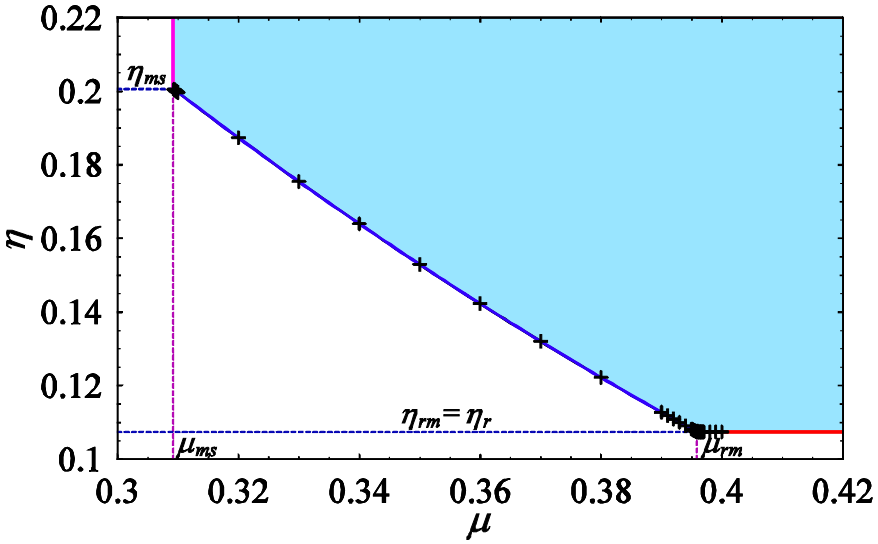

Fig. 3 Least thickness to radius ratio η at variable friction coefficient μ., obtained by analytical and numerical analyses. The mixed sliding-rotational mode range $\mu_{ms} < \mu < \mu_{rm}$ is limited by $\mu_{ms} = 0.309215$ ($\varphi_{ms} = 17.1824°$) and $\mu_{rm} = 0.395832$ ($\varphi_{rm} = 21.5952°$). The shaded region represents possible equilibrium states of couples (μ,η)

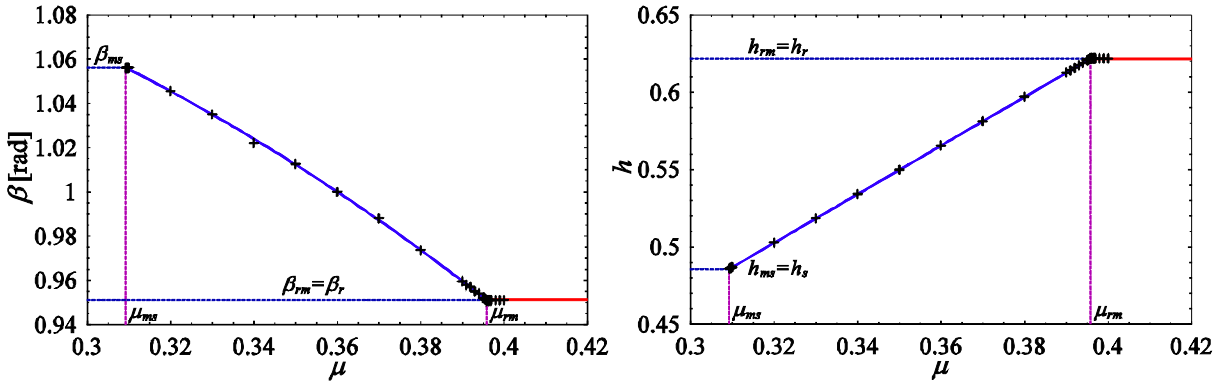

Fig. 4 Trends of characteristic parameters β, h at variable friction coefficient μ, obtained by analytical and numerical analyses: (a) inner hinge angular position β; (b) non-dimensional horizontal thrust h

At transition $\mu = \mu_{rm} = 0.395832$ ($\varphi_{rm} = 21.5952°$), a first sliding joint appears at the shoulder ($\beta = \alpha = \pi/2$), for a non-dimensional horizontal thrust $h = h_r$ matching $h = h_\mu(\mu) = \alpha\mu = \pi/2\ \mu$. This marks the transition from purely-rotational to mixed sliding-rotational collapse mechanisms. The simultaneous presence of a hinge and a sliding joint at the shoulders is detected in both analytical and numerical analyses. The 2-dof collapse mechanism in such transition state could be represented by any linear combination of 1-dof mechanisms in Figs. 1b and 1c.

When μ is then further decreased from μ_{rm}, thrust h keeps fixed by friction as $h = h_\mu(\mu)$. The least thickness required for equilibrium is forced to increase. Indeed, since a lower μ is related to a lower resistance to sliding, a larger section (thickness) is needed in order to prevent collapse. Also, the purely-rotational collapse mechanism cannot be triggered further, since a thickness larger than η_r (independent on μ) is needed to avoid sliding. Hence, the collapse mode that appears first, when thickness is decreased from a super-critical value to the critical one, is the mixed sliding-rotational mechanism in Fig. 1c. At the same time, the inner hinge at the haunches moves further down, at decreasing μ, from the location at purely-rotational collapse. This is due to the non-linear increasing trends of η and β at lowering h (fixed here by friction) from the purely-rotational solution [7].

At $\mu = \mu_{ms} = 0.309215$ ($\varphi_{ms} = 17.1824°$) an additional sliding joint opens-up at $\beta_{ms} = 0.499796\ rad = = 28.6362°$, when $\eta = \eta_{ms} = 0.200637$, with $h = h_{ms} = 0.485714$. At $\eta = \eta_{ms}$, this sliding joint coexists with a hinge at the haunches at $\beta_m(\mu_{ms}) = 1.05616\ rad = 60.5134°$, and the corresponding 2-dof mixed collapse mode would be any linear combination of 1-dof modes in Figs. 1c and 1d. Any larger value of $\eta > \eta_{ms}$ would instead represent limit equilibrium conditions at $\mu = \mu_{ms}$ for which purely-sliding

collapse would develop (Fig. 1d). In practice, at $\mu = \mu_{ms}$ any value $\eta > \eta_{ms}$ would correspond to limit states associated to purely-sliding modes in Fig. 1d and the arch is actually no-longer able to stand.
Nothing should be said, by the present static approach, for values of $\mu < \mu_{ms}$, since then equilibrium is no-longer possible at any value of η. Thus, it may be concluded that the shaded region in Fig. 3 represents the equilibrium states of couples (μ,η) allowing for arch equilibrium under self-weight. The inferior boundary of this domain is set by constant line $\eta = \eta_r$ at $\mu \geq \mu_{rm}$, then by curve $\eta = \eta_m(\mu)$ at $\mu_{ms} \leq \mu \leq \mu_{rm}$, finally by vertical line $\eta \geq \eta_{ms}$ at $\mu = \mu_{ms}$ (Fig. 3).

5. CONCLUSIONS

The role that friction coefficient μ at the theoretical joints plays in the definition of geometrical collapse of continuous full semi-circular masonry arches (half-angle of embrace $\alpha = \pi/2 = 90°$) has been investigated. The analytical treatment presented in [6-8] has been extended, by releasing Heyman's hypothesis 3 of friction high-enough to prevent sliding. At decreasing friction coefficient μ, different collapse mechanisms have been located (Figs. 1b-d):

- for $\mu > \mu_{rm}$ classical purely-rotational collapse (Fig. 1b), with five hinges in the symmetric configuration of the whole arch (one at the crown, two at the haunches and two at the shoulders);
- for $\mu_{ms} < \mu < \mu_{rm}$ mixed sliding-rotational collapse (Fig. 1c), with three hinges in the whole arch, one at the crown and two at the haunches, and with two sliding joints at the shoulders;
- for $\mu = \mu_{ms}$ and $\eta > \eta_{ms}$ purely-sliding collapse (Fig. 1d), with four sliding joints in the whole arch, placed symmetrically at the shoulders and at the haunches (at an angle $\beta_s \cong 30°$ differing from that $\beta_m(\mu_{ms}) \cong 60°$ locating the last inner hinge position in the previous collapse mechanism at $\mu = \mu_{ms}$).

At the two transition instances $\mu = \mu_{rm}$ and $\mu = \mu_{ms}$, 2-dof mechanisms that are linear combinations of the two adjacent 1-dof modes above are possible.
The friction range in which the newly-discovered (analytically) mixed sliding-rotational mode occurs is quite narrow, with friction angles between near 22° and 17°. This result obviously holds true for the ideal case of perfectly-holding shoulders. At decreasing friction coefficient μ, thrust h decreases linearly with it, by ranging from h_r to about 0.78 h_r. At the same time, η increases non-linearly from η_r to about 1.87 η_r (critical thickness almost doubles) and β also increases from near $\beta_r \cong 54.5°$ to about $1.11\beta_r \cong 60.5°$. An inner sliding joint then appears at $\mu = \mu_{ms}$ at a different β_s location near 30°.
This theoretical and numerical investigation has enquired the role of friction in Heyman's masonry arch analysis. Focus has been made on the case of a full semi-circular arch ($\alpha = 90°$). The analysis could be generalised to cases of general half-opening angles α, as preliminarily outlined in [10].

ACKNOWLEDGEMENTS

This work has been carried-out at the University of Bergamo, Faculty of Engineering (Dalmine). The financial support by *"Fondi di Ricerca d'Ateneo ex 60%"* at the University of Bergamo is gratefully acknowledged.

REFERENCES

[1] Heyman J. (1977), *Equilibrium of Shell Structures*. Clarendon Press, Oxford.
[2] Heyman J. (1982), *The Masonry Arch*. Ellis Horwood Ltd., Chichester.
[3] Heyman J. (2009), La coupe des pierres. In *Proc. of the 3rd International Congress on Construction History*, Brandenburg University of Technology, Cottbus, Germany, 20-24 May 2009, Vol. 2: 807-812.
[4] Colasante G. (2007), *Sui meccanismi di collasso degli archi in muratura secondo l'analisi limite*. Laurea Thesis in Building Engineering, Advisor Rizzi E., Co-Advisor Cocchetti G., University of Bergamo, Italy, 175 pages.
[5] Rusconi F. (2008), *Analisi numerica per elementi discreti dei meccanismi di collasso degli archi in muratura*. Laurea Thesis in Building Engineering, Advisor Rizzi E., University of Bergamo, Italy, 126 pages.

[6] Rizzi E., Cocchetti G., Colasante G., Rusconi F. (2010), Analytical and numerical analysis on the collapse mode of circular masonry arches. *Periodical of Advanced Materials Research* (ISSN: 1662-8985), 133-134: 467-472.
[7] Cocchetti G., Colasante G., Rizzi E. (2011), On the analysis of minimum thickness in circular masonry arches. *Technical Report SdC2011/01*, University of Bergamo, 105 pages, January 2011. Submitted for publication.
[8] Rizzi E., Rusconi F., Cocchetti G. (2011), Numerical DEM (DDA) analysis on the collapse mode of circular masonry arches. *Technical Report SdC2011/02*, University of Bergamo, 46 pages, March 2011. Submitted for publication.
[9] Frigerio A. (2010), *Sul meccanismo di collasso misto negli archi semicircolari in muratura.* Laurea Thesis in Building Engineering, Advisor Rizzi E., Co-Advisor Colasante G., University of Bergamo, Italy, 130 pages.
[10] Colasante G. (2010), *Sul ruolo dell'attrito nei meccanismi di collasso degli archi circolari in muratura*. Laurea (Master) Thesis in Building Engineering, Advisor Rizzi E., Co-Advisor Cocchetti G., University of Bergamo, Italy, 213 pages.
[11] Ochsendorf J. (2002), *Collapse of Masonry Structures.* Doctoral Dissertation, University of Cambridge, UK.
[12] Ochsendorf J. (2006), The masonry arch on spreading supports. *The Structural Engineer*, 84(2): 29-36.
[13] Milankovitch M. (1907), Theorie der Druckkurven. *Zeitschrift für Mathematik und Physik*, 55: 1-27.
[14] Gilbert M., Casapulla C., Ahmed H.M. (2006), Limit analysis of masonry block structures with non-associative frictional joints using linear programming. *Computers and Structures*, 84(13-14): 873-887.
[15] Sinopoli A., Corradi M., Foce F. (1997), Modern formulation for preelastic theories on masonry arches. *Journal of Engineering Mechanics*, ASCE, 123(3): 204-213.
[16] Sinopoli A., Aita D., Foce F. (2007), Further remarks on the collapse mode of masonry arches with Coulomb friction. *Proc. of 5th Int. Conference on Arch Bridges (ARCH'07)*, Funchal, Madeira, Portugal, September 12-14, 2007, Lourenço P.B., Oliveira D.B., Portela A. (Eds.), Multicomp, Lda Publishers, Madeira, p. 649-657.